Int J Adv Manuf Technol (2014) 73:849–858
DOI 10.1007/s00170-014-5851-2

ORIGINAL ARTICLE

Microstructure and properties of Fe–Al intermetallic coatings on the low carbon steel synthesized by mechanical alloying

A. Canakci · T. Varol · F. Erdemir · S. Ozkaya · H. Mindivan

Received: 22 November 2013 / Accepted: 9 April 2014 / Published online: 9 May 2014

Abstract Fe–Al coating was obtained on low carbon steel substrates using mechanical alloying and subsequent heat treatment. Light optical microscopy and a scanning electron microscope equipped with energy dispersive spectroscopy were used to conduct the microstructure characterization. Mechanical properties of the coatings were evaluated by microhardness measurements and wear tests. The corrosion behavior was determined by potentiodynamic polarization measurements in 3.5 % NaCl solution. The results of the mechanical and corrosion tests showed that the hardness and wear resistance of the coatings decreased with increasing the milling time, while increase in the milling time resulted in a significant increase in the thickness, porosity level, and corrosion resistance.

Keywords Fe–Al coatings · Wear · Mechanical alloying · Corrosion

1 Introduction

Low carbon steel is widely used in a large number of applications including automobile frames, pipelines, ship plates, bridge beams, etc. These applications are driven by manufacturing requirements for their mechanical properties [1]. However, low carbon steel exhibits a low resistance against corrosion, and progressive deterioration of its structure led to rust formation and consequence loss of some of its mechanical properties. Keeping these problems in view an immense effort has been devoted to improve the general corrosion resistance of low carbon steel. Protective coating is the best method of preventing corrosion of carbon steel. There are many surface treatment methods to improve the surface properties of steel and alloy substrates, especially used in the automobile industry. It is well known that mechanical alloying (MA) process, which involves a repeated cold-working, fracturing, and welding, is widely used in order to protect substrate from corrosive environmental effects. The corrosion resistance properties of hard coatings are studied less frequently than mechanical properties, though there are quite a few publications on the MA coating studies [2–4].

For a typical synthesis of coating materials, such as Fe–Al, Ti–Al, and Ti–N intermetallic, powder mixtures were put into a stainless steel or tungsten carbide cylindrical vial with tungsten balls as the grinding media under the protection of an inert gas; the container was then mechanically rotated on its axis at certain speed. The milling process embraces a complex mixture of fracturing, grinding, high-speed plastic deformation, cold welding, thermal shock, and intimate mixing. Potentially, mechanical milling can produce a large range of nanoscaled materials, including nanocrystalline materials, nanoparticles, and nanocomposites [5]. In recent years, some efficient methods were reported to fabricate the fine grain sized metals and alloys, such as mechanical alloying and spark plasma sintering [6, 7]. The MA process makes microstructure refinement and alloy formation. Microstructure refinement may easily result in fine grains within micrometer sized particles [8]. MA method has proved to be an easy tool in order to promote different kinds of solid-state reactions and to create new materials with peculiar properties. Several papers [9–11] has pointed out that the products of the milling process strongly depend on the milling conditions. The energy transfer and consumption also have been analyzed by means of the experimental and the computer simulation. Thus, changing the

A. Canakci (✉) · T. Varol · F. Erdemir · S. Ozkaya
Department of Metallurgical and Materials Engineering, Engineering Faculty, Karadeniz Technical University, Trabzon, Turkey
e-mail: aykut@ktu.edu.tr

H. Mindivan
Department of Mechanical and Manufacturing Engineering, Bilecik Şeyh Edebali University, Bilecik, Turkey

operating conditions will strongly affect the way by which energy is transferred to the powder mixture, thus affects the coating performance of the final products [12].

The beneficial effect of MA on the production of intermetallic coatings has been investigated by some researchers. Mohammadnezhad et al. [13] found that nanostructured Ni–Al intermetallic coatings can be fabricated on the carbon steel substrates by MA process. Zhan et al. [14] explained that MA technique reduced the treatment temperature and duration significantly when compared to the conventional Al pack cementation processes, providing a new approach to industrial diffusion coatings with great energy and time savings. Molladavoudi et al. [15] discussed that phase transformation and structural and morphological evolutions of CoTi intermetallic coating material occurring during the MA process. They revealed that a composite structure with coarse lamellar-like components was formed with the dissolution of Ti in Co in the early stages of MA. Li et al. [16] studied the effects of the milling durations on the formation quality of Ti–Cr and Ti–Cu coatings. They emphasized that the MA process parameter of milling duration was the main factor to influence the thickening process of the Ti–Cr and Ti–Cu coatings. When the other work conditions were determined, the coating thickness increased following the relative extension of milling duration. As shown in previous studies [13–16], MA method has been used for production of intermetallic coatings. However, to our knowledge, the effect of MA on the corrosion and wear resistance of Fe–Al coatings has not been investigated. Therefore, the purpose of this work is to produce the Fe–Al coating by MA and to investigate effect of milling time on the coating thickness, microhardness, wear, and corrosion resistance of Fe–Al coatings. Since the properties of the obtained coating depend strongly on the milling time [17, 18], the correlation between this parameter and coating properties is of crucial importance in order to improve the quality of the obtained coating for different applications, where this is the aim of this first study.

2 Experimental

In this research work, low carbon steel AISI 1018 was used as a substrate material for MA. The steel coupon was cut into small pieces, each with the dimensions of 12×12×3 mm. The sample surfaces were mechanically polished using 240 to 1,200 grit papers in sequence. Then the samples were rinsed in acetone, ethanol, and water for 5 min, respectively, by an ultrasonic cleaner in order to degrease and clean the surfaces to improve the adhesion of the coating. The surface-prepared samples and Al2024 powders were used as raw materials for deposition. A planetary ball mill with a 200-rpm rotating speed was selected. No process control agent (PCA) was added to the powder, and the milling process was performed in an argon atmosphere. The milling process was carried out in a Fritsch "Pulverisette 7, Premium line" planetary ball mill for up to 12 h using a tungsten carbide bowl and balls (10 mm in diameter). To prevent atmospheric contamination, the milling chamber was completely sealed; if the container was not properly sealed, the atmosphere surrounding the container leaked into the container and contaminated the powder. The heat treatment was carried out in an argon environment to prevent oxidation of the coating systems. The samples were placed in the furnace, which was evacuated of air, filled with argon and heated at 5 °C min^{-1}. The samples were held for 120 min at 600 °C, and then, they were cooled down in the furnace (cooling rate, 5 °C min^{-1}) to minimize the internal stresses. The phase analysis of composite layer was evaluated by X-ray diffraction (XRD; Rigaku Corporation, Japan) using CuKα radiation (1,54059 A°) operating at 30 mA and 40 kV. The XRD patterns were recorded in the 2θ range of 0–100° (step size 0.02° and time per step 1 s).

The microstructure and surface morphology of coatings were evaluated by a scanning electron microscopy (SEM) using the Zeiss EVO LS10 microscope. All cross-sectional microstructures were examined in backscattered (BSE) mode. The coating thickness was measured from all sample sides using a TIME Group coating thickness gauge (TT211), and the average thickness was calculated for each sample. The cross-sections for detailed microstructural observations were prepared using a light optical microscope. Vickers microhardness was determined using microhardness tester (Wolpert) with a load of 0.025 kg and an indentation time of 10 s. The average of 5 indents was used to ensure acquisition of a reasonably representative value. All indents were kept away from porous locations. Microhardness measurements were carried out in the cross-section of the both coating and steel substrate.

Wear behavior of the coatings was determined on a reciprocating wear tester by rubbing a 10-mm steel ball under a normal load of 1 N at normal atmospheric conditions (26± 1 °C and 32±1 % relative humidity). Sliding stroke, total sliding distance, and sliding velocity were 0.01 m, 40 m, and 0.0245 ms^{-1}, respectively. After wear tests, the wear tracks were examined using a Mahr stylus profilometer and a SEM. Results of the wear tests were evaluated according to the area loss of the coatings.

Evaluation of the corrosion was determined by potentiodynamic polarization measurement. For the potentiodynamic polarization measurement, machined samples (square cube shaped samples with an average size of 2 mm×2 mm) were mounted on copper rod using epoxy resin for electrical connection, and open surfaces of all samples were cleaned with deionized water followed by rinsing with methanol and then dried. Before potentiodynamic polarization measurements, an initial delay of 45 min was employed in order to measure the open circuit potential between working and reference

electrodes. Corrosion tests were conducted within a range of ±500 mV of open circuit potential at a scan rate of 1 mV/s. Electrolytic corrosion behavior of the samples was evaluated according to corrosion potential and corrosion current density. Each data point for potentiodynamic polarization tests represents at least an average of three different measurements. After corrosion tests, surface roughness values and 2D surface topography profiles were obtained using a Marsurf PS profilometer.

3 Results and discussion

3.1 Microstructure of Fe–Al coatings

MA is a powder processing technique used to synthesize a variety of non-equilibrium and equilibrium materials starting from blended elemental and compound powders at room temperature in a ball mill [19]. The technique involves repeated cold welding, fracturing and rewelding, resulting in the formation of refined powders of homogeneous chemical composition. In ductile systems, the impact of the grinding balls causes the metal powders to flatten and get work hardens. The flattened layers overlap and form cold welds. As the process continues, the surface of the milling balls and the inner walls of the container are continuously impacted by the balls and powder particles, resulting in coating by the milled powder [20, 21]. While a thin layer is beneficial in preventing excessive wear of the milling medium, a thick layer results in structural in homogeneity and it is difficult to detach from the surface. On the other hand, the process can also be used to produce surface coatings on ball milled components [22, 23]. During the milling, centrifugal forces are produced by the vials rotating around their own axes and by the support disk orbiting around the central axis. The forces are then exerted on the balls, powders, and substrate to be ground. Since the vials and the supporting disk rotate in opposite directions, the centrifugal forces alternately change their directions. Under this condition, the balls are primarily carried up the inner surface of the vials and then run down the inside wall, producing a so-called "friction effect" on the inner wall. Subsequently, the balls, the powders and the substrate material being ground are propelled off the inner wall and travel freely across the inner chamber of the vial, colliding against the opposite inside wall. In this situation, another new mechanism, a so-called "impact effect," is developed during the interaction. The energy developed through the impacts is several times higher than that for conventional ball mills [24].

In order to explain the significant relationship between the physical and mechanical properties of the coating layer, typical microstructures of the coating layer were shown from in Fig 1. As can be seen in Fig. 1, the coating thickness and porosity increased with the increase in the milling time. The average coating thickness and porosity content of the coating obtained by milling of 6 h were measured as 50 μm and 0.5± 0.1 vol.%, respectively. The steel surface underwent very little change at initial stage of coating process (6 h), and the majority of particles were not cold weld on the steel substrate or ball

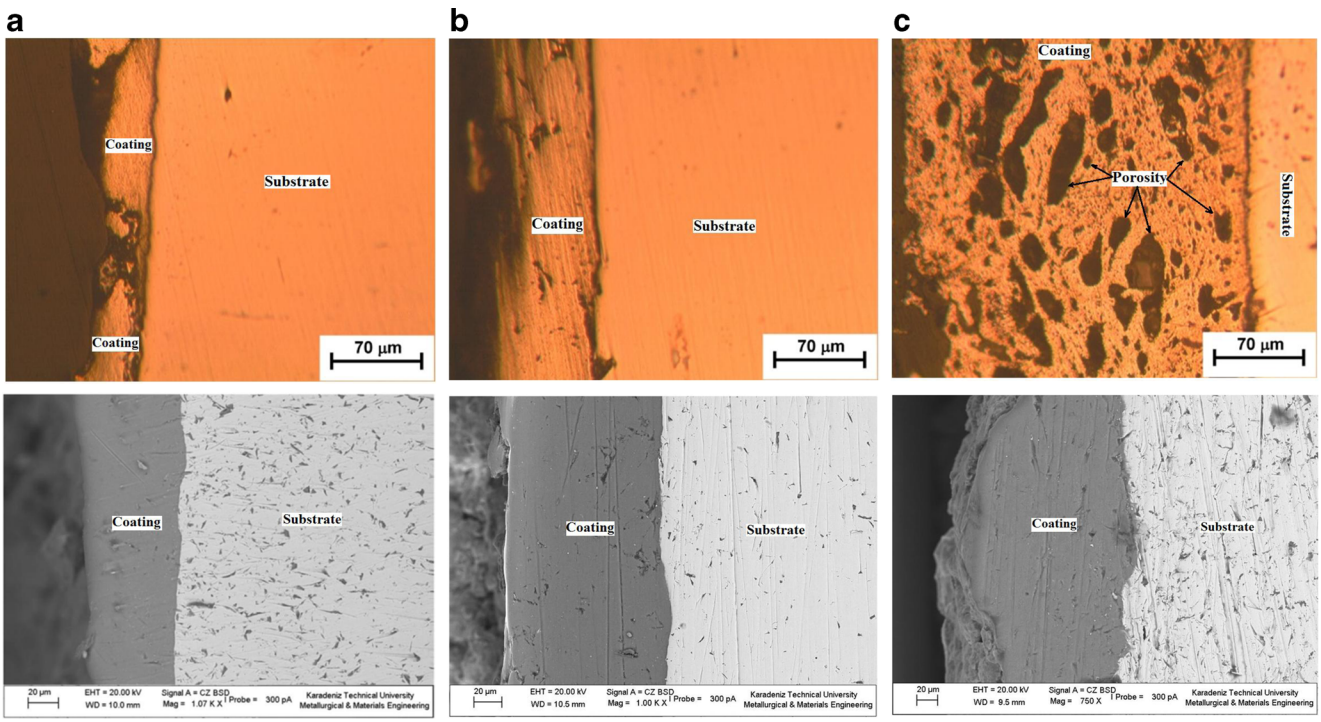

Fig. 1 OM and SEM images of the cross-section of MA-coatings after **a** 6, **b** 9, and **c** 12 h

surface at this stage of the process (Fig. 1a). For a short milling time, the particles were not subjected to an adequate compressive force or kinetic energy input, and therefore, only a minimal coating layer formed on the steel substrate surface [25]. The formation of coating layer could be attributed to the deposition ability of the powder in the cold welded particles region. By increasing the milling time, this ability of the powders increased due to repeated action of cold welding on the steel surface.

When the milling time is 12 h, almost the entire surface was coated with the Al2024 powder (Fig. 1c). The cross-sectional images of the coatings, Fig. 1c, showed that the coating obtained by milling time of 12 h presented higher coating thickness and porosity in comparison with those of the coatings obtained by milling time of 6 and 9 h, indicating that the increase in the milling time increased the flattened particle regions and the formation of a lamellar structure. It is interesting to note that the absence of PCA in the coating process by MA process causes cold welding between ductile Al powders, which influences the properties of the coating layer. Since PCA was not used in coating process, uncoated powders to steel surface cold welded with each other during the initial and second stage of composite coating. In other words, in the absence of PCA, the milling process is dominated by cold welding resulting in a fast increase in particle size of milled powders. The powder which has coarser particle size cannot be participated in the coating process. Although reducing the amount of ductile Al powders involved in the coating process may decrease the coating thickness, coating process should be continued for good microstructure and properties of surface in this stage.

To understand the effect of mechanical alloying on the Fe–Al intermetallic coating, it is necessary to know the change in the structure of the coating layer as a function of milling time. As shown in Fig. 2a, ductile matrix powders changed from a ligament to flake morphology due to plastic deformation in the initial stage of coating process by MA. The distance between deposited ductile powders on the steel substrate was high during this stage. Deposited ductile powders on the steel substrate served as a substrate for new coating layers. At the second stage of the coating process, particle deformation of ductile Al powders and fragmentation due to ball–substrate–ball collisions were the dominant mechanisms. When the milling time increased, ball–powder–ball, ball–substrate–ball, and ball–powder–substrate collisions were accelerated, and the impact energy applied to the coating process was spent generally through the process of fragmentation and plastic deformation of powders. In other words, the coating of ductile powders on the steel substrate is basically controlled by four mechanisms, plastic deformation of the ductile powders, cold welding (powder–powder), deposition on the steel substrate and particle fragmentation due to work hardening. For short milling time, the low plastic deformation and the associated low cold welding were the dominant mechanisms of coating

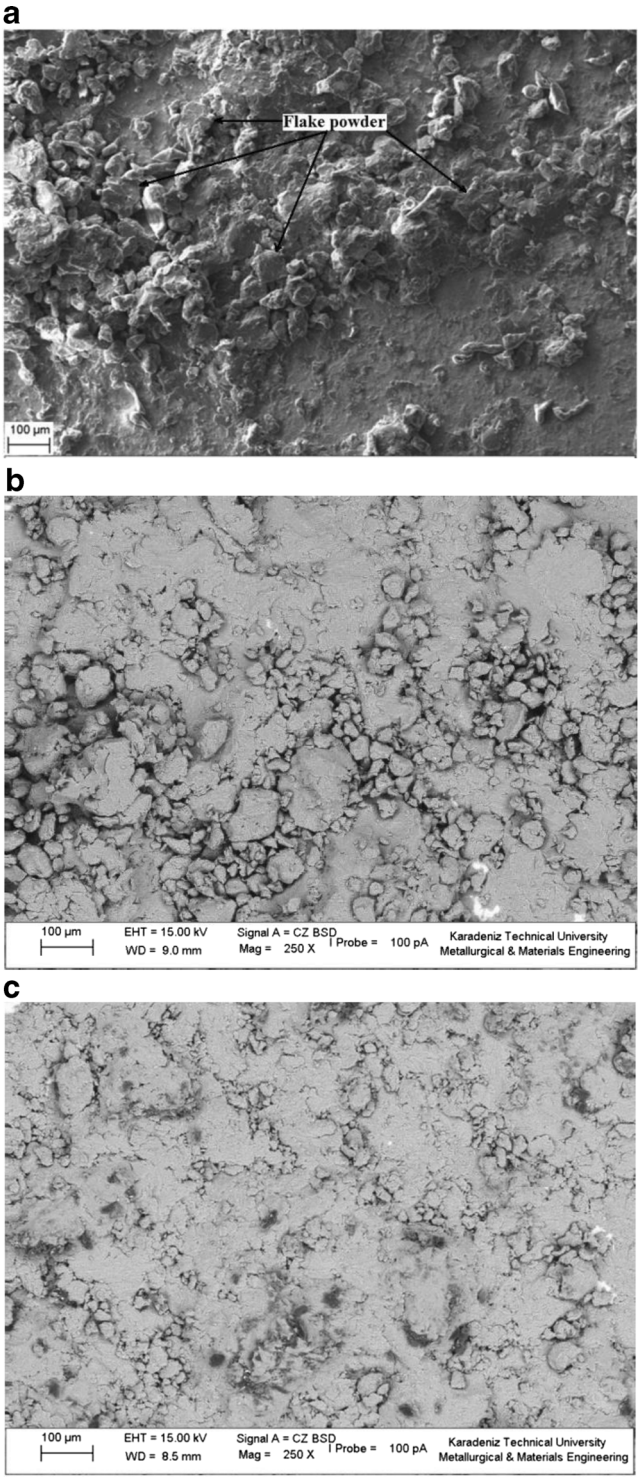

Fig. 2 Surface morphology of the coatings after **a** 6, **b** 9, and **c** 12 h of milling

process, while for the long milling time particle fragmentation and high plastic deformation and the associated high cold welding became the head mechanism. The distance between deposited ductile powders on the steel substrate was reduced due to plastic deformation and new deposited ductile Al

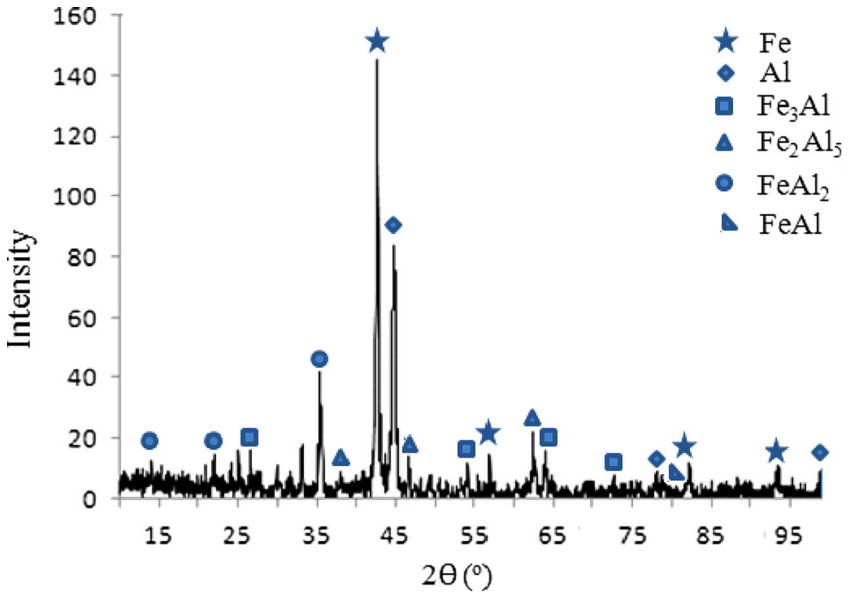

Fig. 3 X-ray patterns of the coating surface

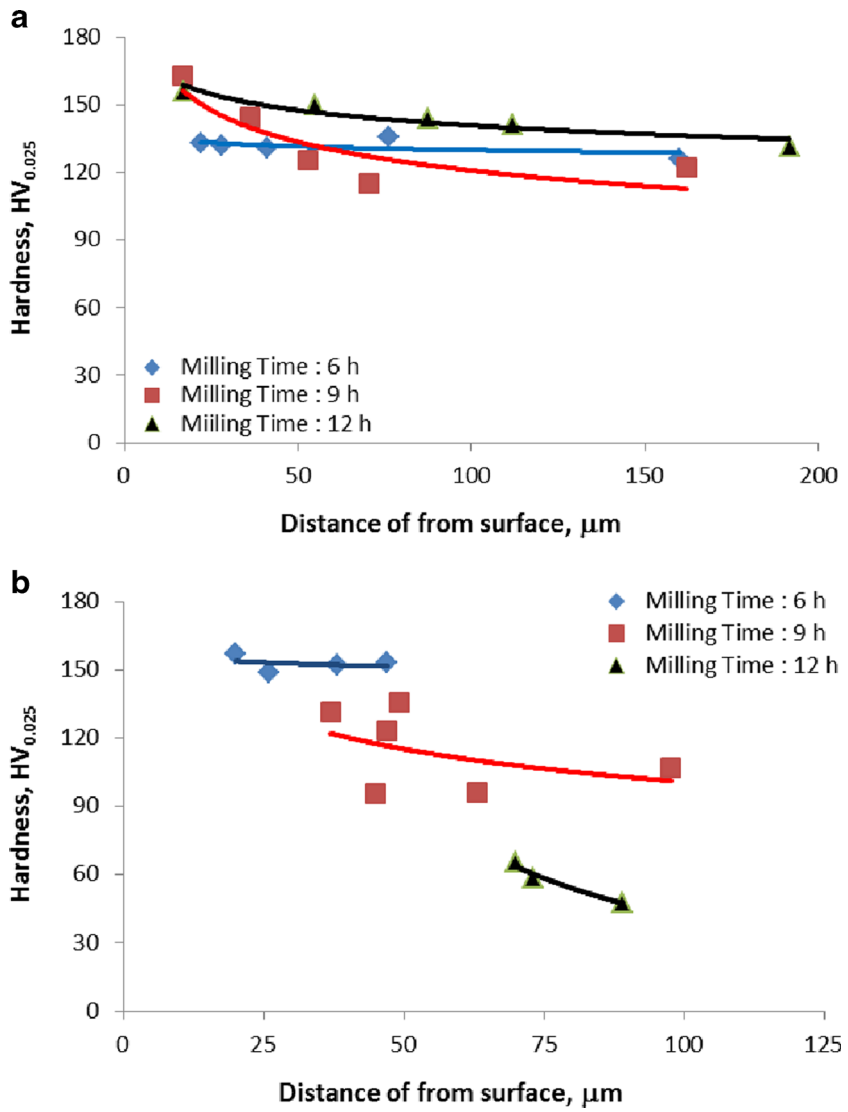

Fig. 4 Microhardness profile of the **a** substrate and **b** coating layer depending on the milling time

powders during the second stage (Fig. 2b). In this stage, it was observed that cold welded powders occurred due to ball–powder–ball collisions during ball milling deposited on the previous coating layer. In the final stage of coating process,

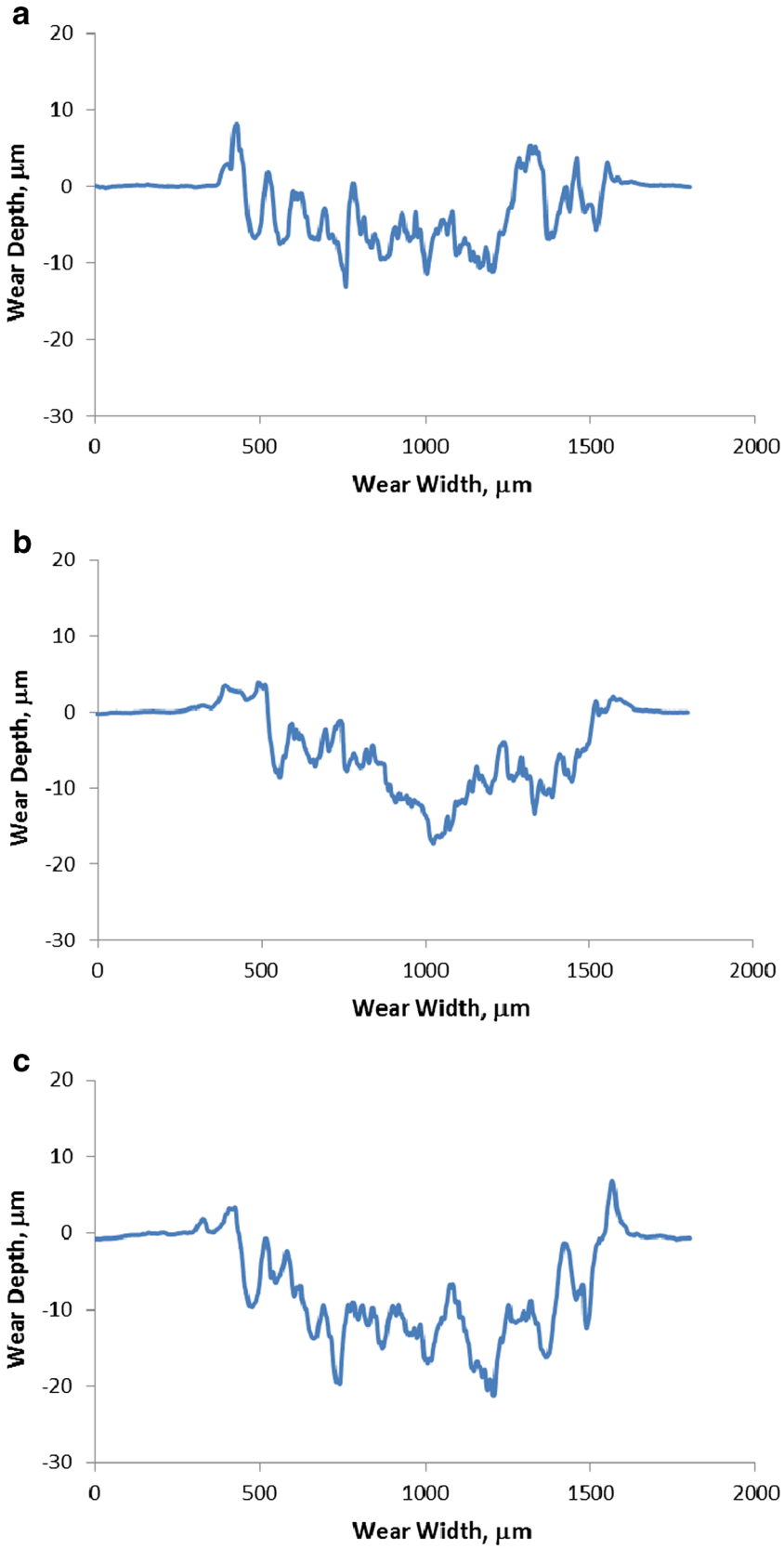

Fig. 5 Surface profiles of worn surface of the coatings obtained by milling time of **a** 6, **b** 9, and **c** 12 h

substrate surface is completely coated by Al2024 powders (Fig. 2c). During this stage, coating thickness was increased with repeated impact effect of balls (Fig. 1c) and a more uniform surface is obtained (Figs. 2c and 3).

3.2 Hardness

Figure 4 shows the hardness variations which have been measured by Vickers microhardness tester for both the substrate and coating layer. Figure 4a showed that the surface hardness of substrate increased with increasing milling time. This can be attributed to deformation effect of ball–substrate–ball collisions. The ball–substrate–ball collision per unit time increased with the increasing the milling time. This increase in the ball–substrate–ball collision frequency resulted in the more deformation of the substrate surface, which increased the substrate hardness (Fig. 4a). This is because the continuous ball impacts during the initial stage of milling should result in the surface hardening of carbon steel substrate via severe plastic deformation before the coating is completely deposited [19]. The hardness of the substrate significantly increased when the distance from surface was lower than 50 μm. The substrate hardness increased to its maximum value at distance of 25 μm and gradually decreased with the increasing distance from surface (Fig. 4a). It is noticeable that the microhardness of coating layer decreased gradually with increasing the milling time (Fig. 4b). This can be attributed to the increasing porosity within coating layer (Fig. 1). With the increase in thickness of the coating obtained at longer milling periods, porosity content between coating layers increased due to irregular packing of Al powders. The coating layer observed at longer milling time was less dense. It should be noted that porosity is a general feature of powder coating process by MA technique and strongly affects hardness of coating layer. With an increase in milling time, porosity increased and so hardness decreased (Fig. 4b).

3.3 Wear

Figure 5 shows the profiles of the worn surface of the coatings with different porosities. It was noticed that the coating with low porosity content showed excellent wear resistance. However, high porosity deteriorated the wear resistance significantly, which hampered the use of the coating. The wear out area of the coating with high porosity (Fig. 5c) was

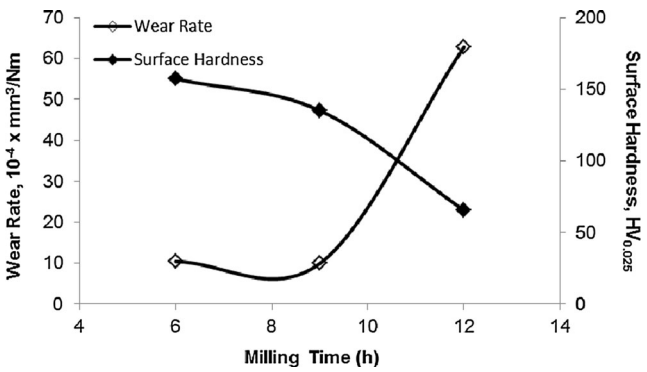

Fig. 6 Wear rate versus hardness of the coatings

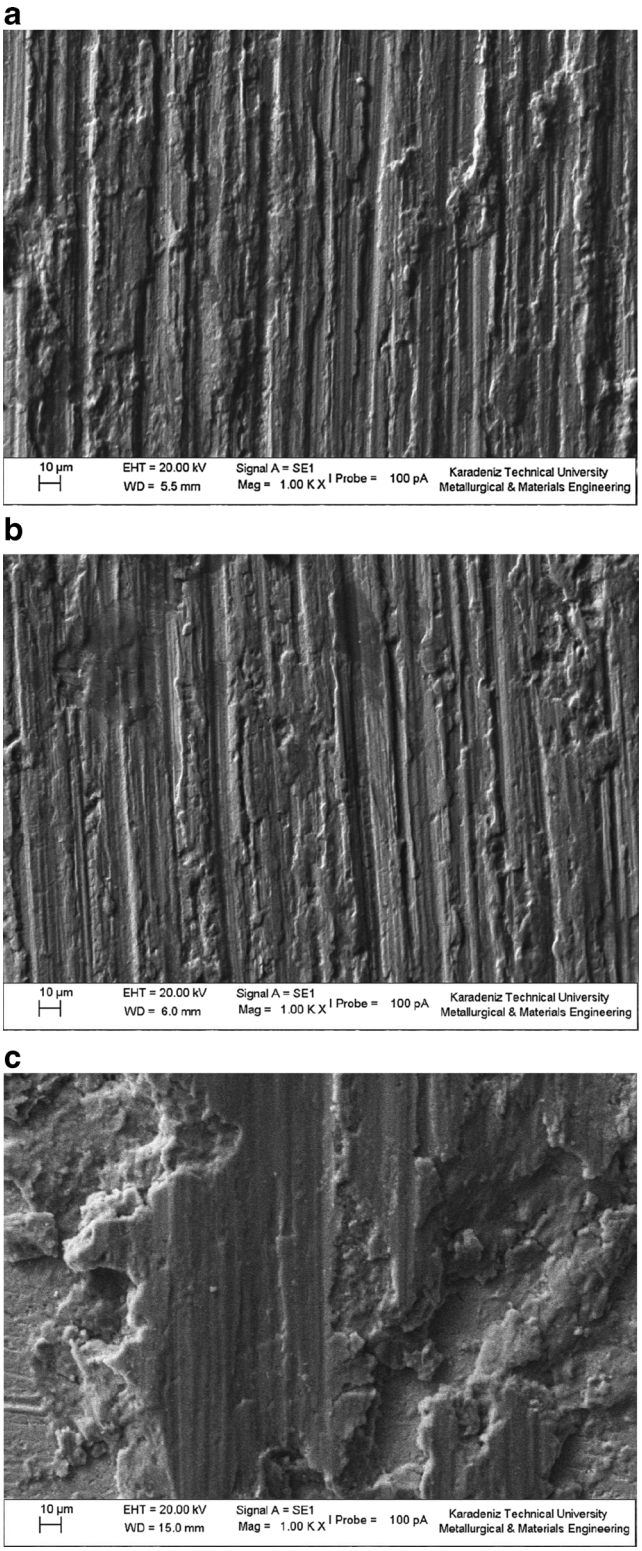

Fig. 7 SEM images of the worn surfaces of the coatings obtained by milling time of **a** 6, **b** 9, and **c** 12 h

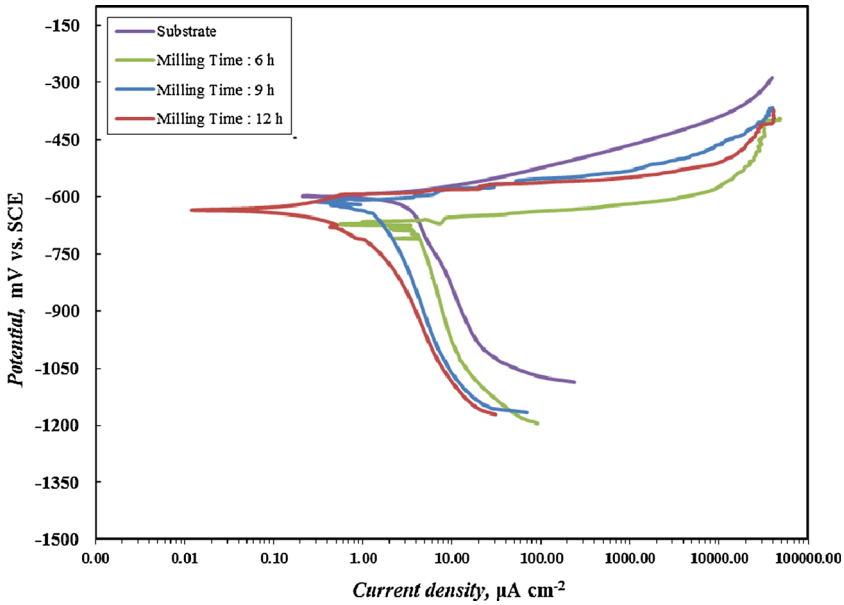

Fig. 8 Potentiodynamic polarization curves of the coatings

about 6 times those of the coatings with low porosity (Fig. 5a, b).

Figure 6 depicts the correlation between the coatings' surface hardness and wear rate. An increase in wear rate values with increasing milling time was observed. Higher wear rate values can be attributed to their lower hardness values and higher porosity content. Among the coatings, the coatings obtained by milling time of 6 and 9 h exhibited higher wear resistance when compared to the coating 12 h. It is clearly revealed that the hardness and porosity played an important role on the wear rate.

Figure 7 shows the SEM images of the worn surfaces of the coatings. SEM examination of the worn surfaces revealed that smoother wear tracks were obtained after wear tests performed on the coatings with low porosity compared to that of the high porosity. It was characterized by the presence of the mechanically mixed layer (MML) on the worn surface of the coatings with low porosity. However, the pores beneath the worn surface would hamper the formation of continuous MML and can propagate significantly. In the presence of porosity, a continuous MML is difficult to form, which is detrimental to the improvement of wear resistance. The existence of the MML is favorable to the improvement of wear resistance, which inhibits the onset of greater wear damage. This is in accordance with the reported results that the MML has a lubrication effect, resulting in the reduced wear.

3.4 Corrosion

The potentiodynamic polarization curves of the substrate and coatings are shown in Fig. 8. The most critical parameters such as corrosion potential (E_{corr}), and current density (i_{corr}) values obtained from this curves are summarized in Table 1. The E_{corr} values of the coatings increased positively due to the formation of a lamellar structure with increasing the milling time. For example, for the coating obtained at 12 h milling period, it was measured to be ~40 mV. Meanwhile, the corrosion current density of the coating produced by the milling time of 12 h was 0.399×10^{-6} A cm^{-2}, approximately ten times lower than that of the coating produced by milling time of 6 h (4.27×10^{-6} A cm^{-2}). In other words, the formation of the lamellar structure dependent on the milling time causes more noble corrosion potentials and lower corrosion current density when compared to those of the thinner coatings produced by a short milling time. It is assumed that the presence of a minimal coating layer formed on the steel substrate surface by the short milling time was able to allow a higher velocity of electrolyte penetration through the coating, which promoted the attack of the steel substrate. Formanek et al. [26] reported that similar observation for NiAl(Cr)–Al_2O_3 coatings and attributed their observation to the formation of a lamellar oxide structure inhibiting the corrosion processes.

Table 1 Corrosion potential (E_{corr}), and current density (i_{corr}) values of the substrate and coatings

	Substrate	Milling time (h)		
		6	9	12
E_{corr} (mv)	−598	−673	−616	−634
I_{corr} (A/cm$^2\times10^{-6}$)	4.45	4.27	1.18	0.399

3.5 Surface roughness

Figure 9 illustrates roughness pictures of the coatings after electrochemical tests. It is obvious that depth of pits on the whole surface of the coating with the milling time of 12 h does not exceed 6 μm (Fig. 9c) while at shorter milling periods of 6 and 9 h depth of pits can even exceed 10 μm (Fig. 9a, b). The polarization test results lead directly to the conclusion that the corrosion resistance of the coating with the milling time of 12 h was better than those of the coatings at 6 and 9 h, which was in good agreement with the results of surface profile measurements.

4 Conclusions

The results of this study can be stated as follows:

1. The MA coatings were successfully produced on low carbon steel substrate without any discontinuity at the coating/substrate interface.
2. According to the XRD patterns of the coatings beside the main phase of Al, there are no other phases in the coatings. It can be concluded that no phase transformation occurs during MA.

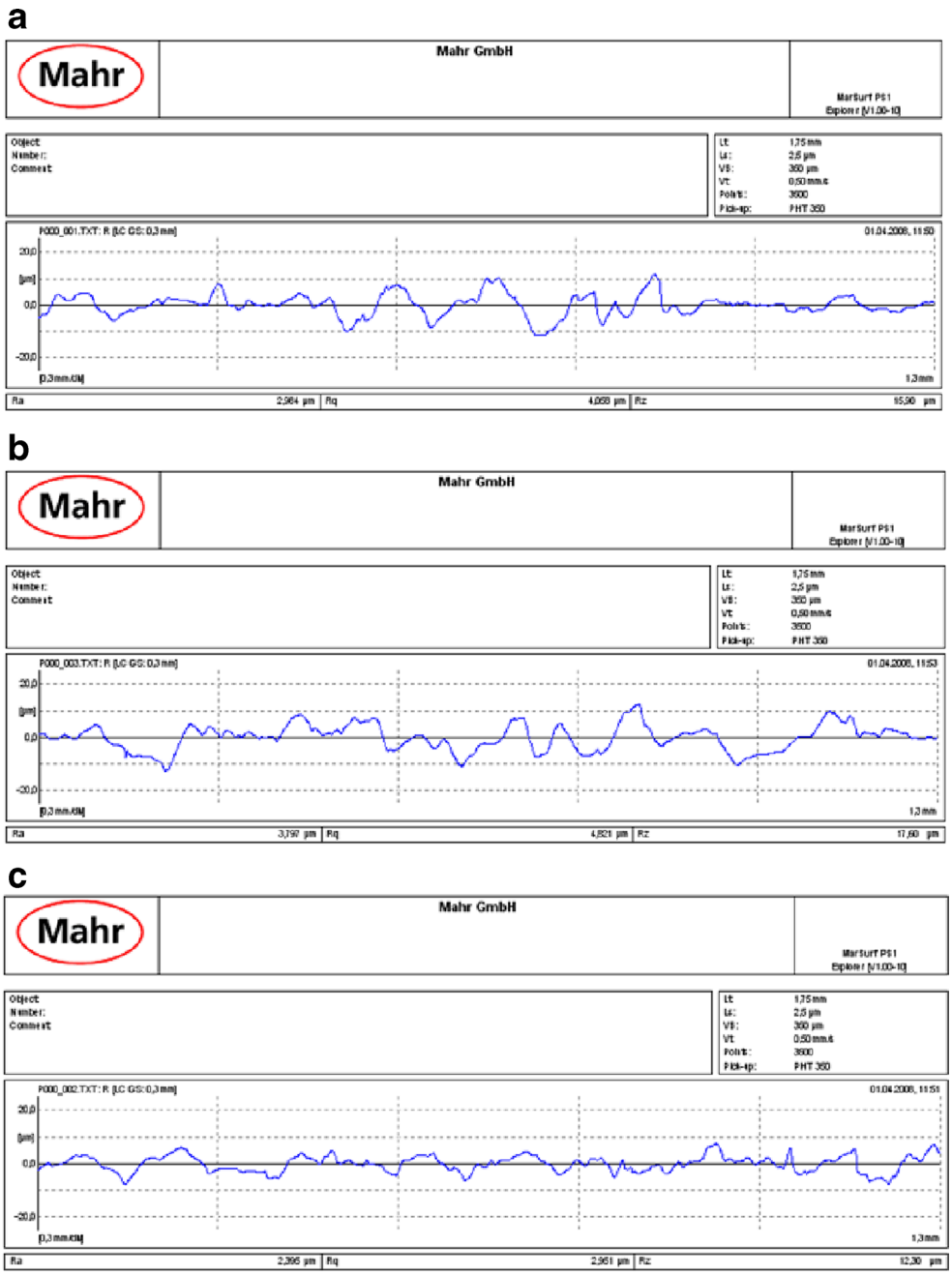

Fig. 9 Roughness of the coatings with the milling time of **a** 6, **b** 9, and **b** 12 h after electrochemical tests

3. The substrate milled for 12 h exhibited much higher hardness in comparison with the substrate milled for 6 h due to severe plastic deformation and strain hardening of the substrate. However, the increase in milling time decreased the hardness of the coatings. The hardness values of the coatings moderately decreased as the volume content of porosity retained in the coating increased.
4. Porosity had a significant influence on wear resistance of the coatings. The coatings with low porosity showed excellent wear resistance, while high porosity lead to a larger wear rate than the coatings with low porosity.
5. It was observed that the coating structure was an effective parameter on the corrosion resistance. It was shown that corrosion resistance increased with the formation of the lamellar structure on the substrate.

References

1. Wang CJ, Chen SM (2006) The high-temperature oxidation behavior of hot-dipping Al–Si coating on low carbon steel. Surf Coat Technol 200:6601–6605
2. Gupta G, Mondal K, Balasubramaniam R (2009) In situ nanocrystalline Fe-Si coating by MA. J Alloys Compd 482:118–122
3. Jiang J, Wang Y, Zhong Q, Zhang L (2011) Preparation of Fe_2B boride coating on low-carbon steel surfaces and its evaluation of hardness and corrosion resistance. Surf Coat Technol 206:473–478
4. Jiang J, Wang Y, Zhong Q, Zhou Q, Zhang L, Zadorozhnyya V, Kaloshkin S, Kaevitser E, Romankov S (2011) Coating of metals with intermetallics by MA. J Alloys Compd 509:507–509
5. Zhang D, Cai R, Zhou Y, Shao Z, Liao XZ, Ma ZF (2010) Effect of milling method and time on the properties and electrochemical performance of $LiFePO_4$/C composites prepared by ball milling and thermal treatment. Electrochim Acta 55:2653–2661
6. He Q, Jia C, Meng J (2006) Influence of iron powder particle size on the microstructure and properties of Fe3Al intermetallics prepared by mechanical alloying and spark plasma sintering. Mater Sci Eng, A 428:314–318
7. Paris SE, Gaffet E, Bernard F, Munir ZA (2004) Spark plasma synthesis from mechanically activated powders: a versatile route for producing dense nanostructured iron aluminides. Scripta Mater 50: 691–696
8. Suryanarayana C (2001) Mechanical alloying and milling. Prog Mater Sci 46:1–184
9. Canakci A, Varol T, Ozsahin S (2013) Analysis of the effect of a new process control agent technique on the mechanical milling process using a neural network model: Measurement and modeling. Meas 46: 1818–1827
10. Canakci A, Varol T, Nazik C (2012) Effects of amount of methanol on characteristics of mechanically alloyed Al-Al_2O_3 composite powders. Mater Technol 27:320–327
11. Varol T, Canakci A (2013) Effect of particle size and ratio of B4C reinforcement on properties and morphology of nanocrystalline Al2024-B4C composite powders. Powder Technol 246:462–472
12. Kim J, Satoh M, Iwasaki T (2003) Mechanical-dry coating of wax onto copper powder by ball milling. Mater Sci Eng, A 342:258–263
13. Mohammadnezhad M, Shamanian M, Enayati MH, Salehi M (2013) Influence of annealing temperature on the structure and properties of the nanograined NiAl intermetallic coatings produced by using MA. Surf Coat Technol 217:64–69
14. Zhan Z, He Y, Wang D, Gao W (2006) Low-temperature processing of Fe-Al intermetallic coatings assisted by ball milling. Intermetallics 14:75–81
15. Molladavoudi A, Amirkhanlou S, Shamanian M, Ashrafizadeh F (2012) The production of nanocrystalline cobalt titanide intermetallic compound via mechanical alloying. Intermetallics 29:104–109
16. Li B, Ding R, Shen Y, Hu Y, Guo Y (2012) Preparation of Ti-Cr and Ti-Cu flame-retardant coatings on Ti-6Al-4 V using a high-energy mechanical alloying method: A preliminary research. Mater Des 35: 25–36
17. Nouri A, Hodgson PD, Wen C (2011) Effect of ball-milling time on the structural characteristics of biomedical porous Ti–Sn–Nb alloy. Mater Sci and Eng C 31:921–928
18. Zadorozhnyya V, Kaloshkin S, Kaevitser E, Romankov S (2011) Coating of metals with intermetallics by mechanical alloying. J Alloys Compd 509:507–509
19. Farahbakhsh I, Zakeri A, Manikandan P, Hokamoto K (2011) Evaluation of nanostructured coating layers formed on Ni balls during mechanical alloying of Cu powder. Appl Surf Sci 257: 2830–2837
20. Lu K, Lu J (2004) Nanostructured surface layer on metallic materials induced by surface mechanical attrition treatment. J Mater Sci Eng A 375–377:38–45
21. Revesz A, Takacs L (2007) Coating metals by surface mechanical attrition treatment. J Alloys Compd 441:111–114
22. Romankov S, Sha W, Kaloshkin SD, Kaevitser K (2006) Fabrication of Ti-Al coatings by mechanical alloying method. Surf Coat Technol 201:3235–3245
23. Romankov S, Kaloshkin SD, Hayasaka Y, Komarov SV, Hayashi N, Kasai E (2009) Effect of process parameters on the formation of Ti–Al coatings fabricated by mechanical milling. J Alloys Compd 484: 665–673
24. Suryanarayana C, Ivanov E, Boldyrev VV (2001) The science and technology of mechanical alloying. J Mater Sci Eng A 304–306:151–158
25. Lee H, Lee S, Shin H, Ko K (2009) Mechanical matching and microstructural evolution at the coating/substrate interfaces of cold-sprayed Ni, Al coatings. J Alloys Compd 478:636–641
26. Szczucka-Lasota B, Formanek B, Hernas A, Szymanski K (2005) Oxidation models of the growth of corrosion products on the intermetallic coatings strengthened by a fine dispersive Al_2O_3. J Mater Process Technol 164–165:935–939